Heliyon 10 (2024) e35069

Contents lists available at ScienceDirect

Heliyon

journal homepage: www.cell.com/heliyon

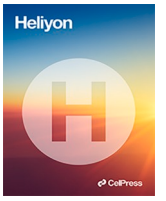

Research article

Development and evaluation of nanoemulsion gel loaded with bioactive extract of *Cucumis melo* var. *agrestis*: A novel approach for enhanced skin permeability and antifungal activity

Ambreen Akhter [a], Jafir Hussain Shirazi [a,**], Haji Muhammad Shoaib khan [a,*], Muhammad Delwar Hussain [b], Mohsin Kazi [c]

[a] *Department of Pharmaceutics, Faculty of Pharmacy, The Islamia University of Bahawalpur, Bahawalpur, 63100, Punjab, Pakistan*
[b] *Department of Pharmaceutical Sciences, School of Pharmacy, University of Maryland Eastern Shore, Princess Anne, MD, 21853, USA*
[c] *Department of Pharmaceutics, College of Pharmacy, King Saud University, P.O. Box-2457, Riyadh, 11451, Saudi Arabia*

A R T I C L E I N F O

Keywords:
Nanoemulsion
Cucumis melo var. *agretis*
Carbopol 940
Nanoemulsion gel
Antioxidant activity
In vitro permeation
In vitro antifungal activity

A B S T R A C T

The utilization of phytoconstituents in skin care products has emerged as a notable trend due to their recognized safety and therapeutic efficacy. However, the challenge lies in improving the effective delivery of phytoconstituents to specific tissues, primarily attributed to their poor solubility and low permeability. This study endeavors to address this challenge by developing, optimizing and characterizing *Cucumis melo* var. *agrestis* (CME) extract loaded nanoemulsion gel (CME-NEG), aiming to enhance the skin permeability and antifungal activity. Herein, nanoemulsions encapsulating the plant extract were prepared using ultrasonication technique and were characterized for droplet size, zeta potential, polydispersity index (PDI) and entrapment efficiency. Further, Fourier transform infrared spectroscopy (FTIR) and scanning electron microscopy (SEM) analysis were conducted to characterize the optimized CME extract loaded nanoemulsion (CME-NE 3) formulation. The optimized formulation was blended with Carbopol 940 gel to develop CME-NEG, which was evaluated for release kinetics, *in vitro* permeation and *in vitro* antifungal activity. High performance liquid chromatography (HPLC) analysis confirmed the presence of gallic acid, chlorogenic acid, 4-Hydroxy benzoic acid (HB acid), kaempferol, caffeic acid and quercetin. Findings of 2,2-diphenyl-1-picrylhydrazyl (DPPH) assay showed that the ethanolic extract had highest antioxidant activity (88.88 %). The optimized formulation displayed smooth spherical nanodroplets with size of 175.5 ± 1.56 nm, zeta potential of −21.5 ± 0.12 mV, PDI of 0.192 ± 0.06, and highest entrapment efficiency (EE) of 91.35 ± 1.65 %. The release profile of CME-NE exhibited a controlled release characteristic and the release kinetic mechanism was best described by the Korsmeyer-Peppas (Kp) model. In a 24 h permeation study, it was observed that the *in vitro* permeation of CME-NEG was 58.63 %, significantly higher than that of CME extract loaded plain gel (CME-PG) with an enhancement ratio of 2.12. The prepared CME-NEG formulation also presented enhanced antifungal activity as compared to pure CME extract. In conclusion, the designed CME-NEG offers a promising topical drug delivery system with enhanced skin permeability and antifungal activity.

* Corresponding author.
** Corresponding author.
E-mail addresses: ambreen.iub@gmail.com (A. Akhter), jafir.shirazi@iub.edu.pk (J.H. Shirazi), shoaib.khan@iub.edu.pk (H.M. Shoaib khan), mdhussain@umes.edu (M.D. Hussain), mkazi@ksu.edu.sa (M. Kazi).

https://doi.org/10.1016/j.heliyon.2024.e35069
Received 21 April 2024; Received in revised form 19 July 2024; Accepted 22 July 2024
Available online 24 July 2024

List of abbreviations

Abbreviations	Full forms
CME	Cucumis melo var. agrestis
ECME	Ethanolic fraction
CHCME	Chloroform fraction
HCME	n-Hexane fraction
TPC	Total phenolic content
TFC	Total flavonoid content
NE	Nanoemulsion
P-TPD	Pseudoternary phase diagram
CME-NE	Cucumis melo var. agrestis extract loaded nanoemulsion
CME-NEG	Cucumis melo var. agrestis extract loaded nanoemulsion gel
CME-PG	Cucumis melo var. agrestis extract loaded plain gel
EE	Entrapment efficiency
HB Acid	4-Hydroxy benzoic acid
PDI	Polydispersity index
FTIR	Fourier transform infrared spectroscopy
HPLC	High performance liquid chromatography
SEM	Scanning Electron Microscopy
DPPH	2,2-diphenyl-1-picrylhydrazyl
KP model	Korsmeyer-Peppas model

1. Introduction

Skin is the vital and largest organ of human body that protects against chemicals, environmental pollutants and harmful radiations coming from the sun [1]. It also plays a vital role to maintain electrolytes and preventing water loss from the body [2]. Dermatological disorders like candidiasis and dermatophytosis are prevailing worldwide and considered as the main global burdens in treatment of various diseases [3,4]. Fungal infections affecting the skin particularly involve Candida species, which are the most common fungi for superficial skin infections [5]. These infections initially affect the skin superficially but can progress to deeper layers through desquamation, highlighting the need for therapeutic agents capable of penetrating deep into the skin for effective treatment [6]. Various conventional synthetic antifungal drugs are used to treat fungal infections but their repeated use cause potential allergies and resistance. To address this, plant derived bioactive compounds are being explored as a promising alternative therapeutic strategies with profound antifungal properties [7].

Over the decades, natural products are being used by humanity for health benefits. Phytochemicals like secondary metabolites (phenolic and flavonoids compounds) found in various plants provides immunity and protection from damages caused by exposure to solar radiations, inflammatory disorders, cardiac and neurodegenerative diseases, also provide defense against bacterial, fungal and viral infections [8]. In current metabolomics studies various analytical techniques like FTIR, HPLC, LC-MS, GC-MS and NMR are being employed for the exploration of plants secondary metabolites, among these MS and NMR based techniques are most recent for identification and quantification of the metabolites to develop new therapeutic agent [9,10]. According to earlier studies, natural phyto-antioxidants such as quercetin, gallic acid and catechin play a vital role in the treatment of these dermatological disorders due to their remarkable therapeutic potential [11]. Topical application of the therapeutic agents has been an alternative route of administration to conventional systems. Topical delivery of pharmaceutical agents aids the advantage of improved topical bioavailability due to large surface area of the skin and minimum systemic toxicity [12]. In topical delivery of phytobioactive constituents, stratum corneum present the major challenge to their permeation and topical bioavailability profile due to their relatively large molecular size, low solubility and instability [13]. Due to the hydrophilic nature of these phytobioactive constituents, a lipid environment is needed, or these molecules should be micro or nanosized so that they may easily penetrate through the skin. The development of nano-therapeutics offers opportunities to bridge the gap in the current therapeutic area and enhance the efficacy of conventional synthetic as well as herbal treatment methods [14].

Among the nanotechnology based drug carrier systems such as nanoparticles, liposomes, ethosomes, nanoemulsion has emerged as a promising solution to overcome the constraints of solubility, permeation and to revolutionize the effective delivery of phytobioactive constituents [14,15]. Nanoemulsions are thermodynamically stable colloidal particulate systems with droplet size of 10–200 nm. It consists of two immiscible liquids in which the oily phase containing the hydrophobic drug is dispersed in an aqueous phase, stabilized by a thin layer of surfactants or cosurfactants [16]. They are ideal contenders for encapsulating and delivering hydrophobic and poorly soluble phytochemicals due to their unique characteristics, such as small droplet size, high interfacial area, and improved solubilization capability [17]. This approach holds great potential for enhancing therapeutic outcomes by increasing permeability and reducing adverse effects through simultaneous delivery of polyphenols, possibly with synergistic effects. The tailored design of nanoemulsion formulations with gel system enables controlled release profiles, targeted delivery and enhanced cellular uptake of phytochemicals, resulting in improved therapeutic effects [18]. Nanoemulsion presents versatile options to overcome the lipophilic barriers in dermatology and skincare for treating skin infections. They provide improved stability, better antifungal drug delivery, and improved absorption of therapeutics. Overall, nanoemulsions hold potential for enhancing the efficacy of topical treatments, resolving issues with conventional formulation [19].

Cucumis melo var. *agrestis* (CME) belongs to the Cucurbitaceae family and is generally known by the names chibber, small guard, wild musk melon, and kachri and is cultivated worldwide. It has a pivotal role in preventing cancer prevalence and as an antioxidant, anti-inflammatory and antimicrobial agent [20]. Researchers are much more interested in quantifying the bioactive phytoconstituents that function as free radical scavengers and have an effective defense against malignant and degenerative diseases. Hence, the use of natural phytoantioxidants to formulate drug products free from synthetic ingredients is gaining popularity due to their efficacy and safety [21]. The phytochemical profile of *Cucumis melo* var. *agrestis* from the Cholistan desert of Bahawalpur, Punjab, Pakistan, and its extract-loaded nanoemulsion gel formulation have not been investigated for dermatological applications. The study is very important since *Cucumis melo* var. *agrestis* may have unique phytoconstituents that have advantages for skincare. Our study fills this information gap and offers a novel method to skincare formulations that utilize *Cucumis melo* var. *agrestis* unrealized potential for dermatological applications. This is a significant contribution to the pharmaceutical sector. This study adopts a novel approach to delivering phytoconstituents for skincare by developing a CME extract loaded nanoemulsion gel (CME-NEG). The work provides comprehensive characterization, including nanodroplets size and zeta potential, and overcomes problems with low permeability and poor solubility. The nanoemulsion gel demonstrates enhanced antifungal efficacy, improved solubility and skin permeability. The formulation's intriguing potential for improved topical drug administration and HPLC-confirmed phytoconstituents are among its unique features. Therefore, this study aimed to perform phytochemical profiling of CME extract, develop and characterize thermodynamically stable extract-loaded nanoemulsion gel formulation for improving skin permeability and antifungal activity as an innovative topical drug delivery system.

2. Materials and methods

2.1. Chemicals

Clove oil, tween 80, ethanol, n-hexane, chloroform, 2,2-diphenyl-1-picrylhydrazyl (DPPH), Carbopol 940, ascorbic acid, quercetin, gallic acid, Folin-Ciocalteu reagent and triethanolamine were procured from Merck (Germany). Other supplementary chemicals were also of analytical grade unless specified otherwise.

2.2. Authentication and collection of plant

Plant fruits; *Cucumis melo* var. *agrestis* were collected from the cholistan dessert of Bahawalpur, Pakistan, and verified by a taxonomist of the botany department, The Islamia University of Bahawalpur (IUB), Pakistan to obtain a Ref No. 115/Botany for future use. The collected fruits were washed, shade dried and then stored at 25 °C in airtight jars to prevent contamination.

2.3. Phytochemical extraction

The dried plant material (250 g) was ground into powder, soaked in 80 % ethanol at room temperature for 3 days and subjected to solvent extraction 3 times to obtain the maximum yield of phytochemicals. After extraction and filtration steps, the extract was concentrated by using a rotary evaporator (Heidolph, Kelheim, Germany) under reduced pressure at 37 °C. The resultant concentrated extract was weighed after drying, and its yield was calculated to be 55 g. From this, 15 g was preserved as the ethanolic fraction (ECME), while the remaining residue was mixed with deionized water and subsequently subjected to extraction for sequential fractionation using chloroform and n-hexane. The obtained fractions were designated CHCME (18.33 g) and HCME (15.44 g), representing the chloroform and n-hexane fractions of *Cucumis melo* var. *agrestis*, respectively. All fractions were kept in sealed containers and stored in a refrigerator for further analysis.

2.4. Phytochemical investigations

The phytochemical screening of extracts was performed by standard phytochemical techniques [22]. All solvent fractions were screened for the presence of naturally occurring metabolites such as alkaloids, phenols, flavonoids, tannins, saponins, glycosides, carbohydrates, proteins and lipids by using different reagents such as Dragendroff reagent, ferric chloride, ammonia test, lead acetate, froth, Borntrager test, Molish's reagent, Biuret and saponification. For the estimation of bioactive principles, all the investigations were performed in triplicate.

2.5. Fourier transform infrared spectroscopy (FTIR) analysis

FTIR investigation was performed to characterize the ethanolic (ECME), chloroform (CHCME) and n-hexane (HCME) fractions of CME extract for identification of the functional group responsible for its biological activities [23]. The investigations were carried out by applying continual pressure to a small amount of dried plant extract placed on the sample holder. Utilizing the attenuated total reflectance (ATR) mode of a FTIR spectrophotometer (Bruker, Tensor 27 series, Germany), a scanning range of 4000-500 cm^{-1} and % transmittance in the range of 60 %–130 % were produced and analyzed.

2.6. Total phenolic content (TPC)

The Folin-Ciocalteu microplate procedure was employed for estimation of TPC with slight modifications as reported previously [24]. Here, Folin-Ciocalteu reagents (10 % 10 μL) were mixed with 100 μL of (1000 μg/mL) plant extract. The mixture was kept at 37 °C for approximately 10 min to complete the reaction. Then, sodium carbonate solution (15 % 90 μL) was added and allowed to stand at room temperature for approximately 1 h. The absorbance was measured at 765 nm using a Labtech microplate reader (Model LT- 4500). The results of the total phenolic content were expressed in mg GAE (gallic acid equivalent)/g of dried extract.

2.7. Total flavonoid content (TFC)

For quantification of TFC, the aluminum chloride colorimetric method was employed with some modifications that have been mentioned previously [21]. One hundred microliters of plant extract (1000 μg/mL) was mixed with 25 μL of $NaNO_2$ (1 %) solution and 10 μL of $AlCl_3$ (10 %) solution with an interval of 5 min to obtain the reaction mixture. Then, 35 μL of NaOH (1 M) solution was mixed with the reaction mixture after the subsequent addition of 30 μL of absolute methanol. The obtained solution was incubated at room temperature for 30 min. Absorbance was measured at 510 nm using a Labtech microplate reader (Model LT-4500). The results of the TFC were expressed in mg QE (quercetin equivalent)/g of dried extract.

2.8. Quantification of polyphenols by HPLC

High performance liquid chromatography (HPLC) analysis of the ethanolic fraction of CME extract for the determination and quantification of polyphenols was carried out using a method reported previously [25] with slight modifications. Stock solutions of extract (1 mg/mL) were prepared in methanol in amber Eppendorf tubes to protect them from exposure to light and were subsequently filtered through micro filters. HPLC analysis was conducted using a Flexar PerkinElmer System (PerkinElmer, Shelton, CT, USA). The system was equipped with an LC-Shelton CT, gradient model pump system, 06484 (USA) UV/Visible detector, a column oven, and a degasser (DG-20A5) system. A hypersisssl GOLD C18 column (250 × 4.6 mm × 5 μm) from Thermo Fisher Scientific Inc. was utilized. Separation was achieved using a nonlinear gradient composed of acetonitrile: methanol (70:30) and water with 0.5 % glacial acetic acid as the mobile phase. The flow rate of mobile phase was kept constant at 1 mL/minute and injection volume was 20 μL. Polyphenolic contents in the extract were detected at a wavelength of 280 nm. Fresh stock solutions of reference standards were prepared in methanol at a concentration of 1 mg/mL. For preparation of working standards, the stock solutions were diluted with methanol to concentrations ranging from 0.4 to 100 μg/mL. The calibration curve for each standard was generated by plotting the graph between concentration versus corresponding peak area. Identification was performed by comparing the UV–visible spectra of the peaks and the retention times with the reference standards used. Quantification was performed by external standard method using the calibration curves of reference standards.

2.9. In vitro antioxidant activity

The radical scavenging ability of different fractions of CME extract was determined by the DPPH method adopted by Tasneem et al. with some modifications [26]. In detail, 90 μL of DPPH solution (0.2 mM) was thoroughly mixed with 10 μL of extracts at concentration (1000 μg/mL) in a 96-well microplate reader. Then, the solution mixture was incubated for 30 min at 37 °C in the dark. The absorbance of the solutions was recorded at 517 nm using a Labtech microplate reader (Model LT-4500). Ascorbic acid was employed as an antioxidant reference standard. DPPH decolorization is an indication of radical scavenging ability, which was estimated by:

% Inhibition = [(A0-A1)/A0] * 100

A0 = Control Absorbance

A1 = Standard/sample Absorbance

2.10. Development of nanoemulsion (NE) formulations

2.10.1. Screening for nanoemulsion constituents

For nanoemulsion development, the screening of different nanoemulsion constituents for determining the solubility of ethanolic fraction of CME extract was accomplished with the shake flask technique through the addition of excess extract in 2 mL oils, including clove oil, olive oil and isopropyl myristate oil; surfactants, such as Tween 80, Tween 20 and Span 80; and cosurfactants, such as isopropyl alcohol, ethanol and PEG 400 in tightly closed vials. The mixtures were subjected to continuous stirring at 37 °C for 48 h by a magnetic stirrer to obtain uniform dispersion. After 72 h, the mixtures were centrifuged at 10000 rpm for 10 min, and the supernatant was collected. The extract concentration was determined at a wavelength of 235 nm by using UV–Vis spectrophotometer (U-1800, HITACHI, Japan). The constituents with high solubility were selected to outline the phase diagram.

2.10.2. Construction of the pseudoternary phase diagram (P-TPD)

A phase diagram was designed using TernaryPlot.com to determine the appropriate quantities for selected oils and Smix (surfactant: cosurfactant) ratios. The ratios that give the maximum region of the nanoemulsion zone were selected for further utilization in formulation development. It was constructed by the aqueous titration method at ambient temperature. For this purpose, Tween 80 as a surfactant and ethanol as a cosurfactant at a ratio of 2:1 were used as Smix, along with clove oil as an oily phase and water as an aqueous phase. Oil and Smix with different weight ratios, 1:9, 3:7, 5:5, 7:3, and 9:1, were mixed and titrated with water using a magnetic stirrer. After stirring when equilibrium was attained, the formulations were visually observed for transparency, turbidity, ease of flow and phase separation.

2.10.3. Preparation of CME loaded nanoemulsion (CME-NE) formulations

CME-NE formulations were developed using ultrasonication method [27]. Based on the identification of the nanoemulsion zone in the phase diagram, three compositions were chosen. The nanoemulsions were constituted by dissolving the appropriate quantity of CME extract as an active ingredient in the oily phase, and then Smix (2:1) was added to the oily phase and thoroughly mixed under continuous stirring for 20 min. Then, water was added to the mixture with constant magnetic stirring at 1200 rpm at room temperature until homogenous and clear oil in water nanoemulsion formed. After that, the prepared formulations were subjected to ultrasonication for 2 h using ultrasonicator (Elma, E30H Elmasonic, Germany).

2.11. Thermodynamic stability studies of CME-NE formulations

The thermodynamic stability of the CME-NE formulations were investigated by evaluating the samples under various stress conditions: centrifugation, heating cooling cycles, and freeze thaw cycles [28]. The prepared formulations were analyzed for a heating cooling cycle by storing them at 45 °C and then at 4 °C for 48 h at each temperature for three cycles. The samples were subjected to centrifugation (Ultracentrifuge machine, Sigma D-37520, Germany) for 30 min at 3500 rpm and then analyzed for any sign of change in nanoemulsion formulations, such as sedimentation or phase separation. Moreover, the samples were assessed for freeze–thaw cycles by keeping them at −21 °C and then thawed at +25 °C for 48 h at each temperature. These three cycles were conducted, and formulations were examined for any change in the formulations [29]. Those formulations that show transparency, with a single phase and no turbidity under stress conditions, were selected for further investigations.

2.12. In vitro characterization of CME-NE formulations

2.12.1. Determination of droplet size, zeta potential and ploydispersity index (PDI)

To assess the size, charge and homogeneity of nanoemulsion formulations, droplet size, zeta potentials and PDI were determined using a Malvern Zetasizer (Model ZS90, UK). Nanoemulsion formulations were diluted with appropriate dispersants prior to measurements so that an adequate amount of light passed through the samples. The analysis was performed at room temperature, measurements were taken in triplicate, and averages were calculated [30].

2.12.2. Entrapment efficiency (EE)

The percent entrapment efficiency of CME-NE formulations was calculated by using an indirect method reported previously with some modifications [31]. Nanoemulsion formulations were ultracentrifuged at 12000 rpm for 1 h, supernatant was collected and diluted with phosphate buffer saline (PBS) to calculate the concentration of free drug refers to the CME extract. Samples were again centrifuged and the above process was repeated three times. The supernatants were analyzed by UV–Vis spectrophotometer (U-1800, HITACHI, Japan) at 235 nm to determine the concentration of CME extract. The % entrapment efficiency (EE) was calculated as:

$$\% \text{ Entrapment efficiency} = \text{Total drug added - free drug/Total drug added} \times 100$$

2.13. Selection of optimum formulation

The formulation exhibiting the lowest globule size, PDI, EE%, and greatest zeta potential (ZP) was selected as the optimized formulation for further study.

2.14. In vitro characterization of optimized CME-NE formulation

2.14.1. Drug excipient interaction analysis

FTIR analysis was performed to study the interaction between the different constituents of optimized CME-NE formulation using a FTIR spectrophotometer (Bruker, Tensor 27 series, Germany). CME extract, formulation excipients (clove oil, tween 80, ethanol), Blank NE and optimized CME-NE formulation were subjected to FTIR profiling. The ATR (Attenuated total reflectance) mode of the spectrophotometer was run, the analytes were placed on the sample chamber, and the spectral area within the scanning range of 4000-500 cm^{-1} was found and analyzed.

2.14.2. Morphological characterization

Scanning electron microscope (FEI Nova 450 NanoSEM) was used to study the surface morphology of the optimized CME-NE

formulation. Before imaging, the optimized CME-NE formulation was mounted onto aluminum stubs and stored overnight for samples to be dried, and then the sample was coated with gold film. The SEM Scans were taken using voltage (5 kV) at magnification levels of ×500 and X1,000.

2.14.3. Stability studies of optimized CME-NE formulation

The stability of optimized CME-NE formulation was investigated following ICH guidelines. The CME-NE formulation was stored at 4 °C ± 1 and 25 °C ± 1 for 90 days. During this time span, samples were taken at different time intervals (0, 30, 60 and 90 days) and were evaluated for droplet size, PDI, zeta potential and entrapment efficiency to assess any physical instability.

2.15. Development of CME loaded nanoemulsion gel (CME-NEG)

To formulate a topical gel of the optimized CME-NE formulation, Carbopol 940 was used as a gelling agent. An accurately weighed amount of polymer (1.5 %) was dissolved in an appropriate quantity of distilled water to prepare a gel base. The pH of the formulated gel was adjusted to 5.5 with the subsequent addition of triethanolamine. The optimized CME-NE formulation was incorporated in a gel base at a ratio of 1:1 and thoroughly mixed with continuous homogenization to obtain CME-NEG, which was stored for further characterization. Plain gel containing free CME extract solution (CME-PG) was also prepared in the same way.

2.16. Evaluation of CME-NEG

2.16.1. Stability studies

The prepared CME-NEG and CME-PG were subjected to stability studies at specified temperature and relative humidity (RH) conditions, i.e., 8 °C ± 1, 25 °C ± 1, 40 °C ± 1 and 40 °C + 75 % RH ± 1 at various time intervals for 90 days. The study was performed as per The International Council for Harmonization (ICH) guidelines (2003) [32]. During this time span, both formulations were evaluated for organoleptic parameters (i.e. odor, color, liquefaction, microbial growth and phase separation), pH, electrical conductivity, viscosity and spreadability to assess the physical stability and shelf life of the formulations.

2.16.1.1. Organoleptic evaluation. Organoleptic characteristics such as odor, color, liquefaction, microbial growth and phase separation of CME-NEG and CME-PG were investigated by keeping them at different temperatures and relative humidity conditions, i.e., 8 °C ± 1, 25 °C ± 1, 40 °C ± 1 and 40 °C + 75 % RH ± 1 for a time period of 90 days.

2.16.1.2. pH measurement. The pH of the freshly prepared CME-NEG and CME-PG was adjusted within the normal range of skin pH (4.5–6.0), after which the pH of all formulations was measured in triplicate at various time intervals stored at different temperature and relative humidity conditions (already specified) by using a numeral pH meter (WTW pH −197i, Germany) for 90 days.

2.16.1.3. Measurement of electrical conductivity. A numeral conductivity meter (WTW COND -197i, Germany) was used to measure the conductivity of freshly prepared CME-NEG and CME-PG stored at predetermined conditions of temperature and relative humidity at specified time intervals for a duration of 90 days. All measurements were taken in triplicate.

2.16.1.4. Spreadability. Spreadability was measured to determine the formulation ability to uniformly spread upon application over the skin surface. The prepared CME-NEG and CME-PG were evaluated for spreadability at various time intervals stored at different temperature and relative humidity conditions (already specified). To carry out this evaluation, a quantity of 0.5 g of freshly prepared formulation was placed between two glass slides. A defined weight of 500 g was placed onto the slides for 1 min, and then the diameter of the area covered by the spread formulation was measured. This measurement was used to calculate the spreadability value.

Table 1
Qualitative screening of phytochemicals in CME extract.

Phytochemicals	Test Method	Extract Fractions		
		ECME	HCME	CHCME
Alkaloids	Dragendroff reagent	+++	–	+
Phenols	Ferric chloride	+++	++	+
Flavonoids	Ammonia test	+++	++	+
Tannins	Lead Acetate	+++	–	++
Saponins	Froth	–	–	–
Glycosides	Borntrager test	+++	++	–
Carbohydrates	Molish's reagent	+	–	–
Proteins	Biuret	+	+	+
Lipids	Sponification	+	+++	+

The symbols + and – indicate the relative presence and absence of phytochemicals, respectively.
*ECME = Ethanolic fraction, CHCME = Chloroform fraction, HCME = n-hexane fraction.

2.16.1.5. Viscosity. The rheology of the freshly prepared CME-NEG and CME-PG formulations was measured at 25 ± 0.5 °C by using a programmable Brookfield Rheometer (USA DV III ultra, Brookfield rheometer) stored at various temperature conditions (already specified) for 90 days. Rheocalc Version 2.6 software was used for the analysis of shear rate, shear stress and viscosity, and the results were recorded in triplicate.

2.17. In vitro release study

The *in vitro* release study was performed using dialysis membrane (MWCO: 12 K Da, Sigma Aldrich, USA) in phosphate buffer saline (PBS) of pH 7.4 used as receptor medium. The 1 g of CME-NE, CME-NEG and CME extract solution, each containing 6 mg of CME extract were loaded into presoaked dialysis bags and sealed. The dialysis bags were clamped and immersed in 200 mL of PBS containing in the vessel of dissolution apparatus (USP type II, Pharma Test Germany) at 37 ± 0.5 °C and a constant stirring speed was adjusted to 100 rpm. Sink conditions were ensured by measuring the solubility of the CME extract in the receptor medium that should remained below its saturation solubility limit. 1 mL of sample was taken at specific time intervals (0, 0.5, 1, 2, 3, 4, 5, 6, 7, 8, 12, 14, 16, 18 and 24 h) from the receptor medium and replenished with the same volume of fresh PBS having same temperature (37 ± 0.5 °C) and pH (7.4) to maintain the volume. Subsequently, the release of CME extract in PBS was estimated at 235 nm using UV–visible spectrophotometer (U-1800, HITACHI, Japan).

2.18. Release kinetics

To study the release kinetics, the data obtained from *in vitro* release was fitted into various kinetic models such as zero-order, first-order, Higuchi, and Korsmeyer-Peppas (Kp) models. The regression coefficient (R^2) and release exponent (n) values were analyzed using DD solver software (Add-In for MS Excel) to determine the mechanism of CME extract release from the developed formulations. The model presenting the highest of regression coefficient (R^2) value was chosen to be the best fit model.

2.19. In vitro permeation studies

The study protocol for *in vitro* permeation studies was approved by the Institutional Animal Ethics Committee (IAEC), Faculty of Pharmacy, The Islamia University of Bahawalpur, Pakistan (IAEC Ref. No.: PAEC/23/100).

To prepare the rat skin for an *in vitro* permeation study, healthy male Albino rats (200–250 g) of 12–14 weeks were sacrificed, dorsal side was shaved and full-thickness skin was excised. The skin was rinsed with normal saline, dried and the subcutaneous connective tissues were removed surgically, followed by three times washing with isopropyl alcohol to remove adhering adipose tissues. The freshly excised skin was examined for integrity, divided into appropriate size pieces followed by immersing in PBS (pH 5.5) at 4 °C to ensure optimal viability and integrity. The skin was used within 24 h to execute the permeation experiment. *In vitro* permeation study of both CME-NEG and CME-PG was carried out on abdominal skin of albino rats according to the method Asghar et al. with slight modifications [33]. The skin was mounted on Franz diffusion cell (Perme Gear, Inc. No.4G-01-00-15-12, Germany) with a 12 mL receptor volume capacity and a 1.74 cm^2 surface area, where dermal side was facing the receptor compartment and stratum corneum side was facing the donor compartment. The 12 mL of PBS solution with a pH of 5.5 was added to the receptor

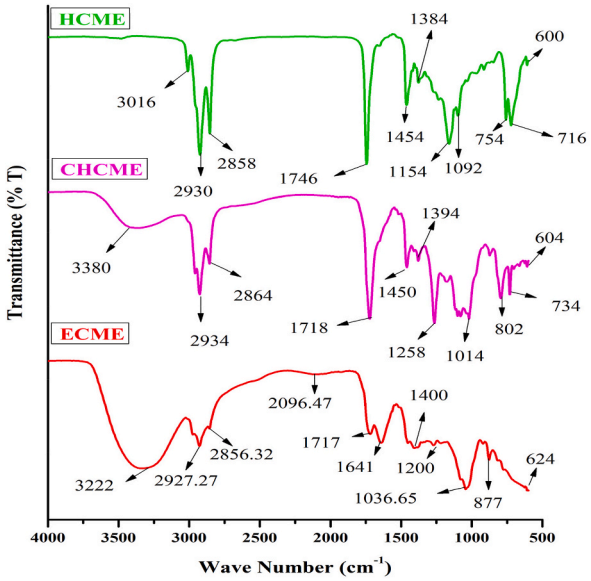

Fig. 1. FTIR spectra of ethanolic (ECME), chloroform (CHCME) and n-hexane (HCME) fractions of CME extract.

compartment of the Franz cell, temperature was set at 37 ± 0.5 °C and constant stirring speed of 300 rpm was maintained throughout the experiment. The experiment was conducted for 24 h. 1 g of each gel containing 6 mg of CME extract was applied via the donor compartment to the skin membrane. Sink conditions were ensured by measuring the solubility of the CME extract in the receptor medium that should remained below its saturation solubility limit. 1 mL of sample was withdrawn at specific time intervals (0, 0.5, 1, 2, 3, 4, 5, 6, 7, 12, 16, 20 and 24 h) from the receptor medium and replenished with an equal volume of fresh PBS having same temperature (37 ± 0.5 °C) and pH (5.5) to maintain the volume. The withdrawn samples were analyzed using UV–visible spectrophotometer (U-1800, HITACHI, Japan) to determine the concentration of permeated CME extract in PBS. The permeation rate of CME extract through the skin was estimated by plotting the % cumulative drug permeation versus time. The following equations were also used to determine the steady state flux and enhancement ratio:

$F = Kp \times Ci \quad E.R. = JF/JC$

Here, F is equal to flux, Kp = permeability coefficient, Ci = initial drug concentration.
Enhancement ratio or E.R., JF = flux of extract-loaded nanoemulsion formulation.
JC = flux of control formulation.

2.20. In vitro antifungal activity

The antifungal activity of the CME extract, blank nanoemulsion gel and CME extract loaded nanoemulsion gel (CME-NEG) against Candida albican ATCC 10231 was evaluated using cup plate method [33]. Sabouraud dextrose media was prepared and sterilized at 121 °C for 15 min in an autoclave. The nutrient media was removed from the autoclave in an aseptic environment and melted media was poured in sterilized petri plates. The growth medium was inoculated with the tested organism and wells were created using a sterilized steel borer. The tested samples were poured in each well and incubate the petri plates for 48 h at 37 °C. Fluconazole was utilized as an antifungal reference standard. The zone of inhibition was measured in millimeters after incubation period of 48 h using graduated scale.

2.21. Statistical analysis

Calculations were carried out in triplicate, and the results are presented as the mean ± standard deviation (S.D.). The outcomes of this study were evaluated using statistical and scientific methods with GraphPad Prism version 8.4.3. Various statistical tools, including ANOVA, paired sample t tests, and correlation analysis, were employed to interpret the findings accurately.

3. Results and discussion

3.1. Phytochemical investigations

Qualitative screening of metabolites is a valuable tool that assists in the identification and characterization of bioactive compounds present in plants. In the present study, different fractions of CME extract were subjected to preliminary screening of phytochemicals to assess the presence of phytoconstituents and the results are shown in Table 1, which are consistent with previously reported studies [34].

3.2. FTIR analysis

FTIR analysis was executed to characterize the ethanolic (ECME), chloroform (CHCME) and n-hexane (HCME) fractions of CME extract for the identification of functional groups. The FTIR spectra of different solvent fractions are depicted in Fig. 1. The major peaks and functional groups observed in the FTIR scan of the ethanolic fraction (ECME) were found at 3222 cm^{-1} (phenolic O–H stretching, N–H stretching) revealing the presence of secondary amines. The peaks at 2927.27 and 2856.32 (C–H symmetric and asymmetric stretching) indicate the presence of alkanes, 2096.47 (C ^ C weak stretching of alkynes), 1717 shows the functional group of carboxylic acid dimers due to C=O stretching, 1641 (C=C stretching of conjugated alkenes, aromatic moiety), 1400 (O–H bending of alcohols), 1200 (C–O stretching of alkyl aryl ethers), 1036.65 (S=O stretching of sulfoxides), 877 (C=C bending of alkenes), and halo compounds were detected at peak 624 cm^{-1}, which shows C-X stretching. The FTIR spectrum of chloroform fraction (CHCME) displayed major peaks at around 3380 cm^{-1} (O–H stretching), 2934, 2864 cm^{-1} (C–H symmetric and asymmetric stretching of alkanes), 1718 cm^{-1}

Table 2
Extract yield, TPC and TFC of plant extract in different organic solvents.

Extract Fractions	Extract Yield	TPC (mgGAE/g)	TFC (mgQE/g)
ECME	55.00 g ± 1.43	98.82 ± 0.03	81.33 ± 0.10
CHCME	18.33 g ± 1.21	61.37 ± 0.05	57.20 ± 0.07
HCME	15.44 g ± 1.25	49.29 ± 0.11	44.97 ± 0.04

*ECME = Ethanolic fraction, CHCME = Chloroform fraction, HCME = n-hexane fraction, TPC = Total phenolic contents, TFC = Total flavonoid contents (Mean ± SD, n = 3).

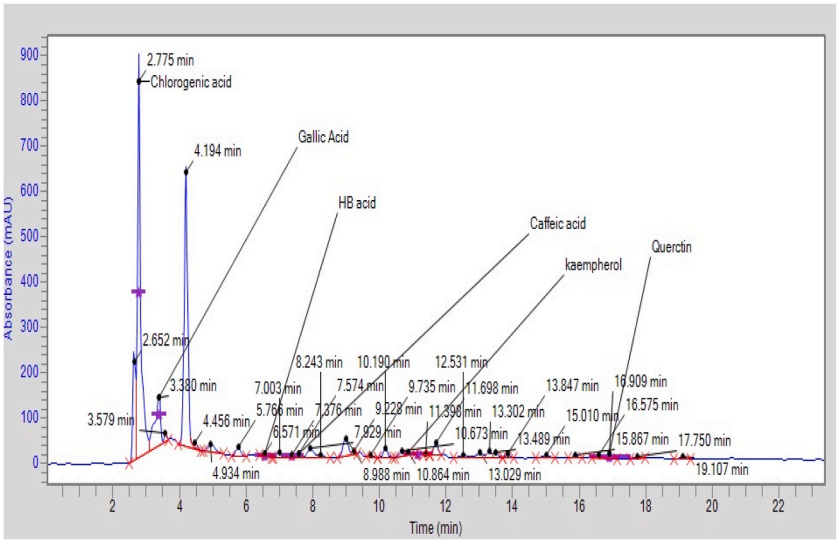

Fig. 2. HPLC chromatogram of ethanolic extract of CME.

Table 3
Quantification of Polyphenols in the ethanolic extract of CME by HPLC.

Compounds	Retention Time (Min.)	Concentration (μg/g)
Chlorogenic acid	2.77	36.43
Gallic Acid	3.38	10.50
HB Acid	6.57	37.85
Caffeic acid	7.57	9.85
Kaempherol	10.86	7.99
Querctin	16.90	12.45

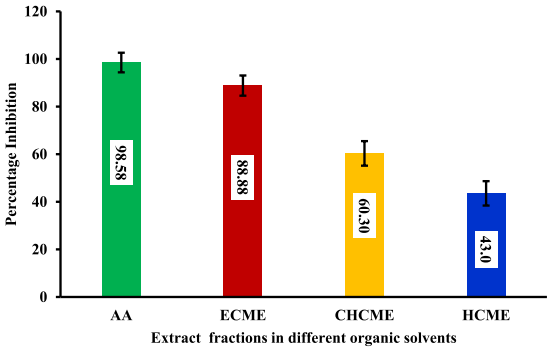

Fig. 3. Radical scavenging activity (% inhibition) of CME extract in different organic solvents and ascorbic acid (standard) * AA = Ascorbic acid, ECME = Ethanolic fraction, CHCME = Chloroform fraction, HCME = n-hexane fraction.

(C=O stretching), 1450 cm^{-1} (C–H bending of alkanes), 1394 cm^{-1} (S=O stretching of sulfates and sulfonyl chloride), 1258 cm^{-1} (C–O stretching of aromatic esters, ethers), 1014 cm^{-1} (C–O, N–H stretching), 802,734,604 cm^{-1} (C–Cl stretching vibrations of halo compounds). FTIR spectrum of n-hexane fraction (HCME) has shown characteristic peaks at around 3016 cm^{-1} (C–H stretching vibration of alkenes) 2930, 2858 cm^{-1} (C–H symmetric and asymmetric stretching of alkanes), 1746 cm^{-1} (C=O stretching due to presence of esters, ketones), 1454 cm^{-1} (C–H bending of alkanes), 1384 cm^{-1} (C–H bending vibrations), 1154, 1092 cm^{-1} (C–N stretching of amines), 754 cm^{-1} (C–H bending), 716 cm^{-1} (C=C bending of alkenes), 600 cm^{-1} (C-X stretching of halo compounds). The FTIR profiling of the *Cucumis melo* var. *agrestis* plant extracts in different solvent fraction has identified a wide range of functional groups, suggesting the plant's potential as a source of different phytobioactive constituents responsible for the diverse medicinal properties.

Table 4
Solubility of CME extract in various surfactants, cosurfactants and oils.

Materials	Solubility (mg/mL)
Oils	
Clove oil	84.40 ± 0.01
Olive oil	63.05 ± 0.05
Isopropyl myristate	46.10 ± 0.03
Surfactants	
Tween-80	56.44 ± 0.014
Tween-20	16.35 ± 0.02
Span-80	28.30 ± 0.04
Cosurfactants	
Ethanol	90.76 ± 0.013
Isopropyl alcohol	40.84 ± 0.024
PEG 400	20.50 ± 0.025

(Mean ± SD, n = 3).

3.3. Quantification of TPC and TFC

We investigated the yield, TPC and TFC of the plant extract in different solvents, and the findings are tabulated in Table 2. The percent yields in different solvent fractions were 55 g ± 1.43 % (ethanol), 18.33 g ± 1.21 % (chloroform) and 15.44 g ± 1.25 % (n-hexane). TPC in the ethanolic fraction was higher (98.82 ± 0.03 mg/g), followed by chloroform (61.37 ± 0.05 mg/g) and n-hexane (49.29 ± 0.11 mg/g), while TFC in ethanol, chloroform and n-hexane was 81.33 ± 0.10, 57.20 ± 0.07 and 44.97 ± 0.04 mg QE/g, respectively. The extraction of phytoconstituents is influenced by various factors, including the polarity of the solvent, ratio of solvent to sample, extraction time and technique [35]. In this study, all variables were constant except for the polarity of the solvents. The ethanol fraction has higher values for yield, TPC and TFC compared to chloroform and n-hexane. The hydro-alcoholic solvent (ethanol) system is an appropriate solvent for the extraction of natural bioactive compounds due to its higher polarity index. These variations correlate with the fact that polar solvents were more effective for the extraction of polyphenolic compounds than nonpolar solvents [36]. The findings of our research are in accordance with previous studies on the variations in polyphenolic quantification using different solvents.

3.4. Quantification of polyphenols by HPLC

HPLC analysis was performed for quantitative and qualitative determination of phenolic and flavonoid compounds. Consequently, different reference standards of polyphenols were utilized, namely, chlorogenic acid, gallic acid, 4-hydroxybenzoic acid (HB acid), caffeic acid, vanillic acid, P-coumaric acid, salicylic acid, coumarin, kaempferol and quercetin. The HPLC chromatogram of the ethanolic fraction shown in Fig. 2 revealed a total of six prominent peaks. The retention times of these peaks closely aligned with the retention times of chlorogenic acid, gallic acid, HB acid, caffeic acid, kaempferol and quercetin. This close correspondence in retention times indicates the presence of these polyphenolic compounds. Table 3 presents the quantified levels of polyphenolic phytoconstituents along with their corresponding relative retention times in the sample. The peak area was employed to estimate the quantity of each polyphenol that was separated using Rp-HPLC. This analysis revealed that HB acid has the highest quantity, followed by chlorogenic acid, quercetin, gallic acid, caffeic acid and kaempferol. The substantial presence of these constituents in such significant quantities validates their appropriateness for dermatological applications, as their presence indicates considerable antioxidant activity.

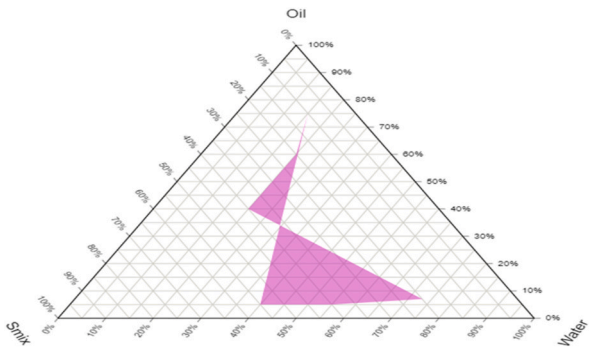

Fig. 4. Pseudoternary phase diagram.

Table 5
Composition of CME-NE formulations.

Nanoemulsion code	Extract (% w/w)	Oil (% w/w)	Smix 2:1 (% w/w)	Water (% w/w)
CME-NE 1	0.6	10	30	59.4
CME-NE 2	0.6	10	35	54.4
CME-NE 3	0.6	10	40	49.4

*CME-NE: *Cucumis melo* var. *agretis* extract loaded nanoemulsion.

Table 6
Thermodynamic Stability of CME-NE formulations.

Nanoemulsion code	Heating–Cooling Cycle	Centrifugation	Freeze–Thaw Cycle	Inferences
CME-NE 1	+	+	+	Pass
CME-NE 2	+	+	+	Pass
CME-NE 3	+	+	+	Pass

3.5. In vitro antioxidant activity

The DPPH assay provides valuable insights into antioxidant potential. Using this method, the free radical scavenging activity of the plant extract in different organic solvents was determined and results are presented in Fig. 3. The ethanolic extract showed the highest antioxidant activity (88.88 %) at a 1000 μg/mL concentration, followed by chloroform (60.30 %) and n-hexane (43.0 %), compared to ascorbic acid, which was used as a standard and had an antioxidant activity of 98.58 %. It has been demonstrated that the polar solvents were more effective for the extraction of polyphenolic compounds than nonpolar solvents [37] and antioxidant potential of plant extracts is proportional to their phenolic contents, indicating a relationship between total phenolic contents and antioxidant activity [38]. The higher polarity of ethanol improves the solubility of polyphenols, making them more bioavailable for interactions with reactive oxygen species (ROS) which in turn contribute to higher antioxidant activity. The superior antioxidant activity of ethanolic extract can be helpful in reducing oxidative stress and to protect skin cells from damage caused by environmental factors such as UV radiation and pollution [39]. In our study, the highest antioxidant potential of the ethanolic extract of CME is due to the presence of a higher concentration of TPC and TFC (Polyphenolic contents) and might be attributed to higher polarity of ethanol as compared to other solvents. Hence it was selected for further studies to develop nanoemulsion gel formulation.

3.6. Development of nanoemulsion (NE) formulations

3.6.1. Screening for nanoemulsion constituents

The solubility of ethanolic fraction of CME extract was assessed in a variety of surfactants, cosurfactants and oils to screen out and select nanoemulsion constituents for developing an optimized and stable formulation. The solubility results are illustrated in Table 4. The choice of the oil phase is critical because it accounts for drug loading and solubility in nanoemulsion systems [40]. Consequently, the solubilizing capacity of three oils, clove oil, olive oil and isopropyl myristate, for phytochemical extract was screened. Among the evaluated oils, the highest solubility was observed in the case of clove oil (84.40 ± 0.01 mg/mL) and hence was selected for developing nanoemulsion formulations. Surfactants along with cosurfactants help in decreasing the interfacial tension by adsorbing at the interface between the two phases and preventing coalescence. Nonionic surfactants are safe due to their hydrophilic nature and are preferred over ionic surfactants, which are mostly associated with toxicity-related concerns [41]. Therefore, in the current study, the nonionic surfactants tween-20, tween-80 and span-80 were screened. The solubility of CME extract was found to be higher for Tween-80 (56.44 ± 0.014 mg/mL) relative to Tween-20 (16.35 ± 0.02 mg/mL) and Span-80 (28.30 ± 0.04 mg/mL); therefore, Tween 80 (14.5 HLB value) was selected for further studies [42]. Whereas, in case of cosurfactants, higher solubility was observed for ethanol (90.76 ± 0.013) and ethanol was selected as a cosurfactant for developing nanoemulsion formulations.

3.6.2. Construction of the pseudoternary phase diagram (P-TPD)

The goal of designing a phase diagram was to develop a stable nanoemulsion formulations. Therefore, a pseudoternary phase diagram was outlined to identify the nanoemulsion zone and the best possible concentration ratios of surfactant, cosurfactant (Smix) and oil [43]. It was designed with extract-free nanoemulsions by using a surfactant: cosurfactant (Smix) ratio of 2:1. Ethanol was used as a cosurfactant in this study, as it has been reported that short chain alcohols (C3–C8) are mostly used as cosurfactants that increase

Table 7
Droplet size, zeta potential, PDI and entrapment efficiency of the CME-NE formulations (mean ± SD, n = 3).

Formulations	Droplet size (nm)	Zeta potential (mV)	Polydispersity Index (PDI)	Entrapment efficiency (%)
CME-NE 1	232.5 ± 3.56	−20.8 ± 0.12	0.216 ± 0.06	85.25 ± 1.25
CME-NE 2	218.9 ± 2.27	−20.3 ± 0.05	0.195 ± 0.10	88.66 ± 1.57
CME-NE 3	175.5 ± 1.56	−21.5 ± 0.12	0.192 ± 0.06	91.35 ± 1.65

the fluidity by reducing the interfacial tension of the interface and enhance the miscibility of the oily and aqueous phases that promote the formation of nanoemulsions [44]. The shaded area of Fig. 4 shows the transparent nanoemulsion zone, whereas the rest of the area indicates turbid or conventional emulsions. Nanoemulsions are transparent due to their characteristic droplet size (20–200 nm) and possess stability against coalescence and sedimentation. Transparency in nanoemulsion formulations is not just an aesthetic preference but also a critical characteristic that indicates the stability [45]. Nanoemulsions that are transparent, have a single phase and show no turbidity, have a longer shelf life than conventional emulsions [46].

Three different formulations were selected from the nanoemulsion region of the phase diagram for the development of nanoemulsion formulations, which are presented in Table 5. It has been reported that the constituents of nanoemulsions may affect various characteristics of nanoemulsion formulations. The CME extract loaded nanoemulsion (CME-NE) formulations were prepared by using different ratios of Smix. The rationale behind the selection of three formulas for the development of nanoemulsion formulations was that we have specifically investigated the concentration dependent effect of Smix (Surfactant: Cosurfactant) on the emulsification efficiency, size reduction, zeta potential, homogeneity and drug entrapment efficiency. Therefore, based on literature survey, three different concentrations of Smix 2:1 (surfactant: cosurfactant) were selected at 5 % intervals, by keeping the selected percentage of oil and extract constant that was reported to produce stable nanoemulsion formulations A literature review revealed that ionic surfactants cause irritation, so the use of nonionic surfactants was preferred at lower concentrations. Therefore, for optimized oil concentration, minimum amounts of surfactant and cosurfactant were selected.

3.7. Thermodynamic stability studies of CME-NE formulations

CME-NE formulations were assessed to check their ability to withstand different stress conditions. The samples were analyzed at various temperatures (4 °C, −21 °C, 45 °C, and 25 °C) to select a stable formulation. The prepared formulations were stable under thermal and mechanical stress as depicted in Table 6. Nanoemulsion formulations that are transparent, have a single phase and show no turbidity under stress conditions were selected and show that they have a longer shelf life than conventional emulsions [46].

3.8. In vitro characterization of CME-NE formulations

3.8.1. Determination of droplet size and PDI

The main critical quality attributes utilized for selection of the optimized nanoemulsion formulations were size of the nanodroplets, PDI and their zeta potential values [47]. The nanodroplets size, zeta potential and PDI results of the developed formulations are presented in Table 7. The nanodroplets sizes for all the studied nanoemulsion formulations were found to be in the range of 232.5 ± 3.56 nm to 175.5 ± 1.56 nm. Among all the nanoemulsion formulations, CME-NE 3 has the smallest nanodroplets, with a particle size

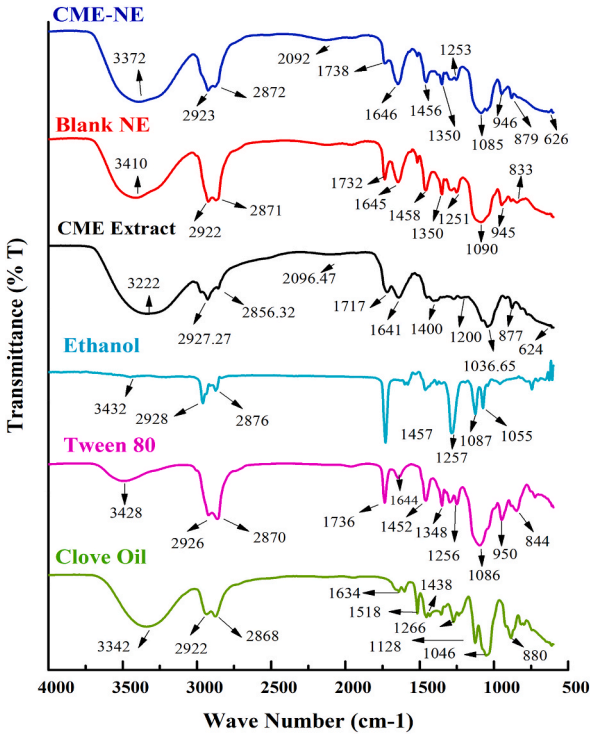

Fig. 5. FTIR spectra of clove oil, tween 80, ethanol, CME extract, blank NE and CME-NE.

value of 175.5 ± 1.56 nm. It has been reported that the concentration of surfactants affects the size and PDI of nanoemulsions [48], and the data presented in Table 7 reveal that the size decreases as the concentration of Smix increases from 30 to 40 %. The reduction in droplet size may be attributed to a larger oil-water interface [49]. Furthermore, the surfactant and cosurfactant contribute to the condensation and expansion of the interfacial film, respectively. The surfactant used in our formulation is Tween 80, which is an ester of long-chain fatty acids that can lead to a decrease in droplet size [50]. The polydispersity index is used to measure the homogeneity or heterogeneity of particle sizes within the formulations [51]. Normal PDI values typically range from 0.0 to 1 [52]. It is reported in literature that PDI values preferably below 0.3 were considered desirable for homogeneous nanoemulsions [53]. The PDI values acquired for all our developed nanoemulsion formulations were below 0.216 ± 0.06, indicating monodispersity and good stability of the formulations.

3.8.2. Zeta potential measurements

The zeta potentials of the studied nanoemulsion formulations shown in Table 7 were found in the range of −20.8 ± 0.12 to −21.5 ± 0.12 mV. The CME-NE 3 formulation showed the highest zeta potential of −21.5 ± 0.12 mV among the developed nanoemulsions. Generally, nanoemulsions with higher zeta potentials are recognized as more stable. However, nanoemulsion developed using nonionic surfactants such as Tween 20/80 are predominantly sterically stabilized rather than electrostatic stabilization mechanism and presents low zeta potential value. we have used Tween 80 as surfactant, which is well accepted steric stabilizer for colloidal systems [54]. The depicted zeta potential values are appropriate to produce stable nanoemulsion formulations.

3.8.3. Entrapment efficiency

The entrapment efficiency of the nanoemulsion is employed to estimate its ability to retain the active ingredient and guarantee its effective delivery to the targeted site. For the studied nanoemulsion formulations, the values of entrapment efficiency ranged from 85.25 ± 1.25 % to 91.35 ± 1.65 %, as presented in Table 7. Among all the nanoemulsion formulations, CME-NE 3 exhibited a higher entrapment efficiency value of 91.35 ± 1.65 %. The composition of the formulation and the nature of the encapsulated phytochemicals within the vesicles are crucial determinants that substantially influence the entrapment efficiency [55]. The literature also reveals that in nanoemulsion formulations, cosurfactants are employed for solubility enhancement, which affects the partitioning of bioactive compounds and consequently impacts entrapment efficiency. On the other hand, as the concentration of surfactant increases, particle size will decrease and the encapsulation efficiency also increases. Herein, the superior entrapment efficiency may be attributed to the higher concentration of Tween-80 and cosurfactant (ethanol) used in the formulation.

3.9. Selection of optimum formulation

Three formulations were developed but CME-NE 3 exhibits the lowest nanodroplets size 175.5 ± 1.56 nm, polydispersity index (PDI) 0.192 ± 0.06, highest entrapment efficiency (EE%) 91.35 ± 1.65 %, and greatest zeta potential (ZP) −21.5 ± 0.12 mV and was selected as the optimized CME-NE formulation for further study.

3.10. In vitro characterization of optimized CME-NE formulation

3.10.1. Drug–excipient interaction analysis

FTIR analysis was executed to investigate the physiochemical interactions between the excipients of the prepared formulation and phytochemicals in the extract. The FTIR spectra of excipients (clove oil, tween 80, ethanol), CME extract, Blank NE and optimized CME-NE formulation are depicted in Fig. 5. The FTIR spectrum of clove oil displayed peaks at around 3342 cm^{-1} (O–H stretching), 2922, 2868 cm^{-1} (C–H stretching vibration associated with aliphatic chains), 1634, 1518 cm^{-1} (C=C stretching vibration of the aromatic moiety) and 1438 cm^{-1} (C–H bending vibrations of –CH2 groups). Signature peaks of clove oil were displayed at around 880-1266 cm^{-1} associated to C=C region. In Tween 80 FTIR spectrum major peaks were found at around 3428 cm^{-1} (O–H stretching), 2926 and 2870 cm^{-}(C–H symmetric and asymmetric stretching of alkanes), 1736 cm^{-1} (C=O stretching of ester group), 1644 cm^{-1} (C=C stretching), 1452, 1348 cm^{-1} (C–H bending vibrations of –CH2 groups). The other bands observed at 1256 & 1086, 950 and 844 cm^{-1} represents C–O stretching and C=C bending vibrations respectively. FTIR spectrum of ethanol has shown broad peak at around 3432

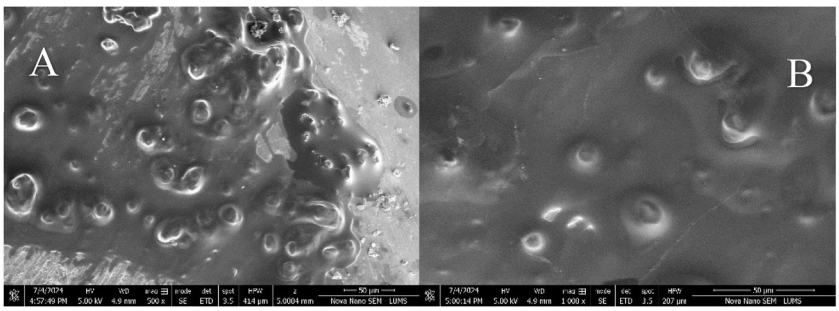

Fig. 6. SEM images of optimized CME-NE formulation at X500 (A) and ×1000 (B) magnification level.

Table 8
Stability studies of optimized CME-NE formulation.

Parameters	Time (Days)	4 °C ± 1	25 °C ± 1
Droplet size (nm)	**0**	175.5 ± 1.56	175.5 ± 1.56
	30	177.3 ± 2.27	177.8 ± 3.71
	60	180.0 ± 2.12	182.3 ± 4.14
	90	181.3 ± 3.56	184.5 ± 2.54
Polydispersity Index (PDI)	**0**	0.192 ± 0.06	0.192 ± 0.06
	30	0.237 ± 0.04	0.245 ± 0.09
	60	0.239 ± 0.03	0.268 ± 0.11
	90	0.240 ± 0.05	0.279 ± 0.07
Zeta potential (mV)	**0**	−21.5 ± 0.12	−21.5 ± 0.12
	30	−21.3 ± 0.15	−21.1 ± 0.34
	60	−21.2 ± 0.19	−20.9 ± 0.26
	90	−21.0 ± 0.17	−20.6 ± 0.37
Entrapment efficiency (%)	**0**	91.35 ± 1.65	91.35 ± 1.65
	30	90.54 ± 1.37	90.48 ± 1.25
	60	89.35 ± 1.65	89.00 ± 1.35
	90	89.12 ± 1.77	88.32 ± 1.57

Table 9
Organoleptic assessment of CME-NEG and CME-PG.

Experimental parameters	Formulation	Color	Odor	Phase Separation	Liquefaction	Microbial growth
Fresh						
Day 1	CME-PG	L	ND	ND	ND	ND
	CME-NEG	LY	ND	ND	ND	ND
After 90 days						
8 °C ± 1	CME-PG	L	–	–	–	–
	CME-NEG	LY	–	–	–	–
25 °C ± 1	CME-PG	L	–	–	–	–
	CME-NEG	LY	–	–	–	–
40 °C ± 1	CME-PG	L	–	–	–	–
	CME-NEG	DY	–	–	–	–
40 °C+75%RH ± 1	CME-PG	L	–	–	–	–
	CME-NEG	DY	–	–	–	–

* Relative humidity (RH); Absent (−); Not detected (ND); Lemon (L); Light yellow (LY); Dark yellow (DY).

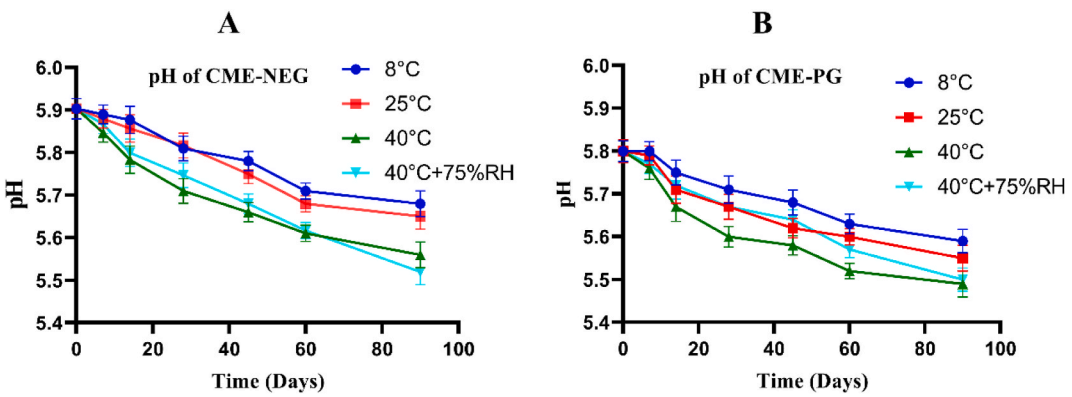

Fig. 7. Change in pH of CME-NEG (A) and CME-PG (B) at varying storage temperatures. A two-way ANOVA and paired sample *t*-test with a 95 % confidence interval revealed significant differences ($P \leq 0.05$).

cm^{-1} associated to O–H stretching of hydroxyl group while peaks at 2928-2876 represents C–H stretching of methyl and methylene group. Furthermore, the peaks in fingerprint region below 1457 cm^{-1} were related to C–C stretching vibrations. The major peaks observed in FTIR spectrum of blank NE (3410, 2922, 2871, 1732, 1645, 1458, 1350, 1251, 1090, 945, 833 cm^{-1}) were related to excipients peaks with no noticeable shift or change. The major peaks observed in FTIR scan of CME extract were found at around 3222 cm^{-1} (Phenolic O–H stretching vibration, N–H stretching of sec amines) [56], 2927.27, 2856.32 cm^{-1} (C–H symmetric and asymmetric stretching of alkanes) [57], 2096.47 cm^{-1} (C ˆ C week stretching of alkynes), 1717 cm^{-1} (C=O stretching of carboxylic acid dimers),

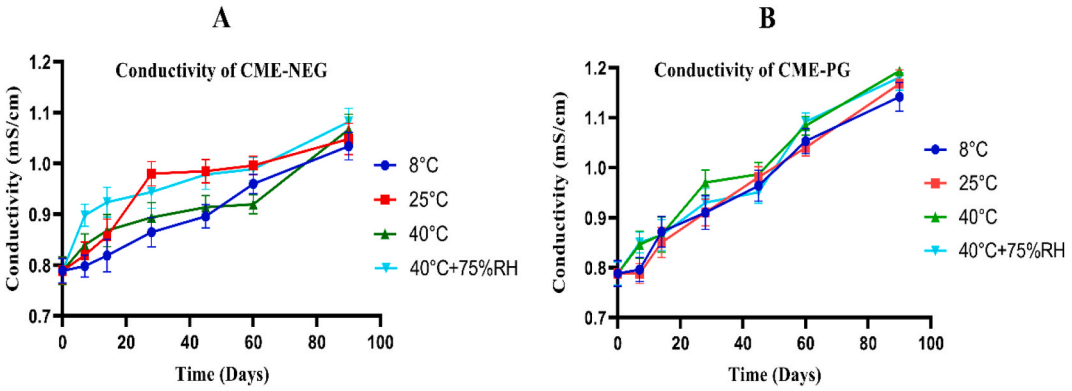

Fig. 8. Variation in electrical conductivity of CME-NEG (A) and CME-PG (B) at varying storage temperatures. A two-way ANOVA and paired sample *t*-test with a 95 % confidence interval revealed significant differences ($P \leq 0.05$).

1641 cm^{-1} (C=C stretching of conjugated alkenes, aromatic moiety), 1400 cm^{-1} (O–H bending of alcohols), 1200 cm^{-1} (C–O stretching of alkyl aryl ethers), 1036.65 cm^{-1} (S=O stretching of sulfoxides), 877 cm^{-1} (C=C bending of alkenes), 624 cm^{-1} (C-X stretching of halo-compounds).The FTIR spectrum of CME-NE formulation has shown that the major functional groups present in CME extract were incorporated into the optimized CME-NE formulation. Moreover, the characteristics peaks of CME extract and excipients remained either unchanged or slightly shifted in the spectrum of CME-NE formulation, the minor shifting of characteristic peaks might be attributed to overlapping of peaks of the CME extract with the strong bands of the excipients in the fingerprint region. These findings confirmed the absence of molecular interactions among the phytobioactive constituents in the CME extract and excipients of the CME-NE formulation.

3.10.2. Surface morphology

The optimized CME-NE formulation was investigated by SEM to obtain information about the surface morphology of nanodroplets in the nanoemulsion. The SEM images taken at X500 and ×1000 magnification are shown in Fig. 6(A and B). The SEM images reveals that most of the nanodroplets were discrete, almost spherical in shape displaying slight irregularities in morphology. The irregularity in shapes and sizes might be attributed to slight agglomeration and sample drying process prior to SEM imaging [58]. The spherical shape of nanodroplets is favorable because it facilitates their penetration through the microscopic pores of the skin [59].

3.10.3. Stability studies of optimized CME-NE formulation

Stability profile of optimized CME-NE formulation stored at 4 °C ± 1 and 25 °C ± 1 for 90 days is presented in Table 8. The results revealed that the optimized formulation remained stable and transparent with no noteworthy alterations in the droplet size, PDI, ZP and entrapment efficiency. Findings of this study shows that CME-NE formulation maintained their stability at storage conditions (4 °C ± 1 and 25 °C ± 1) for 90 days.

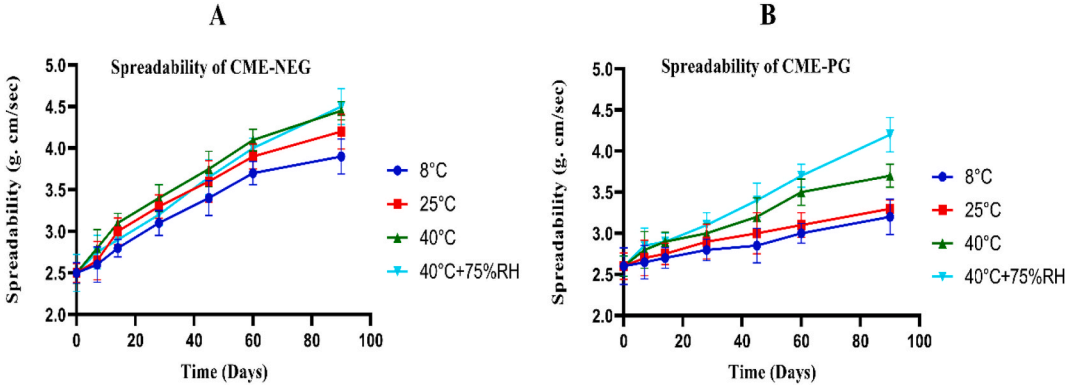

Fig. 9. Change in spreadability of CME-NEG (A) and CME-PG (B) at varying storage temperatures. A two-way ANOVA and paired sample *t*-test with a 95 % confidence interval revealed significant differences ($P \leq 0.05$).

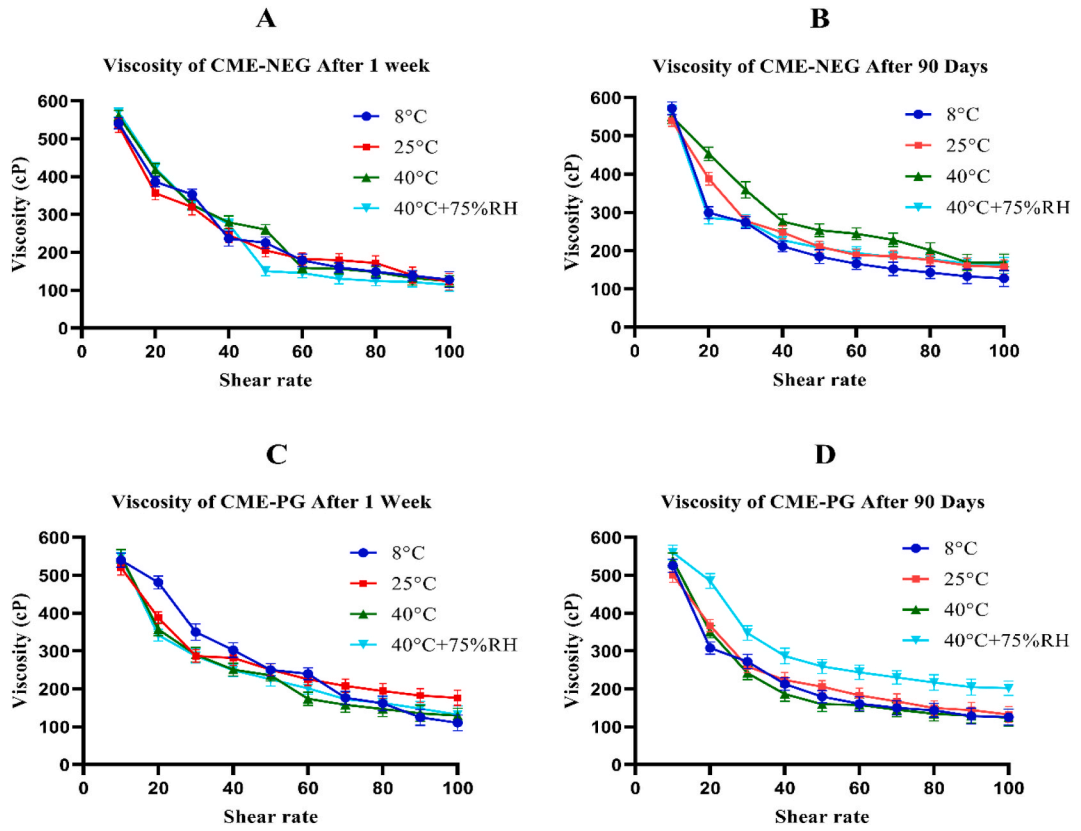

Fig. 10. Variation in viscosity of CME-NEG after 1 week (A) after 90 days (B) and of CME-PG after 1 week (C) after 90 days (D) at varying storage temperatures. A two-way ANOVA and paired sample *t*-test with a 95 % confidence interval revealed significant differences ($P \leq 0.05$).

3.11. Evaluation of CME-NEG

3.11.1. Stability studies

3.11.1.1. Organoleptic evaluation. The findings of the organoleptic assessment are presented in Table 9. A minor change in color was observed in either the CME-NEG and plain gel (CME-PG) stored at 40 °C ± 1 and 40 °C + 75 % RH ± 1. Both formulations have shown no signs of phase separation or liquefaction. This could be attributed to the inclusion of nonionic surfactants, which are known for their ability to remain unaffected by the ionic strength or pH of the integrated agents [50,60]. Throughout the study period, there were no alterations in odor, and no microbial growth was detected, which may be due to the antioxidant properties of the extract, which hinders oxidative deterioration and serves as a natural preservative to inhibit microbial growth. Moreover, the presence of ethanol seems to contribute to this effect synergistically, helping to counteract microbial growth [61].

3.11.1.2. pH measurement. pH is an essential parameter for evaluating the stability and efficacy of skin care products [62]. The slight change in pH values of the CME-NEG and CME-PG are illustrated graphically in Fig. 7(A and B). This depiction reveals a minor decline in the pH of both formulations over a period of 90 days under predetermined temperature conditions. This decrease in pH was most consistent at temperatures of 8 °C ± 1 and 25 °C ± 1. According to previous reports, the pH of the skin ranges from 4.0 to 7.0. However, for cosmeceutical valuation, the pH range of 5.0–6.0 is considered optimal, aligning with the average skin pH [63]. In the present study, the decrease in pH values for both formulations is within the average acceptable range of the pH of skin, which indicates that the formulations show greater stability at lower temperatures, reinforcing their suitability for topical application. The decline in pH may be attributed to the acidic nature of the botanical extract due to the presence of acidic components, which helped to maintain the acidic pH over an extended period of time. Another factor contributing to the decrease in pH is the presence of fatty acids and triglycerides, leading to increased oxidation and hydrolysis, which ultimately causes a decrease in pH [21]. As reported in similar extract-based formulations, the degradation of Tween-80 may be the cause of a decrease in pH under accelerated storage conditions, as its degradation involves the process of hydrolysis and oxidation, which leads to the formation of aldehydes, ketones, fatty acids, epoxides and peroxides, which in turn cause a decrease in the pH of a system [26]. Significant differences in the pH of both formulations were observed ($P \leq 0.05$) at variable times and temperatures when applying a 95 % confidence interval using ANOVA. Furthermore, a paired sample *t*-test intended for multiple comparisons of all samples from both formulations under various storage

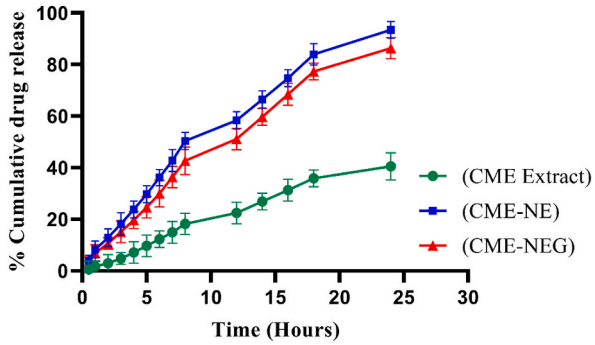

Fig. 11. *In vitro* release profile of CME-NE, CME-NEG and CME Extract solution.

Table 10
Kinetic modeling of release data of CME-NE, CME-NEG and CME Extract.

Formulation	Zero Order (R^2)	First Order (R^2)	Higuchi (R^2)	Korsmeyer Peppas (R^2)	n
CME-NE	0.9269	0.9827	0.9183	0.9881	0.732
CME-NEG	0.8499	0.9817	0.8939	0.9896	0.792
CME-Extract	0.9811	0.9901	0.8412	0.9864	0.907

*n (diffusional release coefficient of Korsmeyer Peppas); *R^2 (correlation coefficient).

conditions showed a significant difference with a correlation coefficient (r) of 0.962.

3.11.1.3. Determination of electrical conductivity. Determination of electrical conductivity is an important parameter for the assessment of formulation stability by measuring the amount of free ions present in a system [64]. The conductivities of the freshly prepared CME-NEG and CME-PG were 0.788 mS/cm and 0.789 mS/cm, respectively. Over an investigational period of 90 days, at predefined storage conditions, a slight increase in conductivity was observed, particularly at 40 °C and 40 °C + 75 % RH, as shown in Fig. 8(A and B). This slight increasing trend in the values of conductivity at higher temperatures may be associated with increased globule size and coalescence of oil droplets of nanoemulsion in the system [24,65]. Significant differences in the conductivity of both formulations were observed ($P \leq 0.05$) at variable times and temperatures when applying a 95 % confidence interval using ANOVA. Furthermore, a paired sample *t*-test intended for multiple comparisons of all samples from both formulations under various storage conditions showed a significant difference, demonstrating a correlation coefficient (r) of 0.909. In the present investigation, there was no considerable change in the conductivity values of the CME-NEG and CME-PG, so it might be considered that both formulations were stable under the studied storage conditions.

3.11.1.4. Spreadability. The spreadability of gel formulations holds significance, as this parameter helps in evaluating the therapeutic efficacy and quantity of the formulation needed for uniform application on the skin [66]. The results of the spreadability of the investigated formulations are shown in Fig. 9(A and B). A minor increase in spreadability was observed over a period of 90 days. Various studies have concluded that viscosity exhibits an inverse relationship with spreadability; an increase in viscosity results in lower spreadability [62]. The findings of the current study showed an increase in spreadability, which is attributed to the decrease in

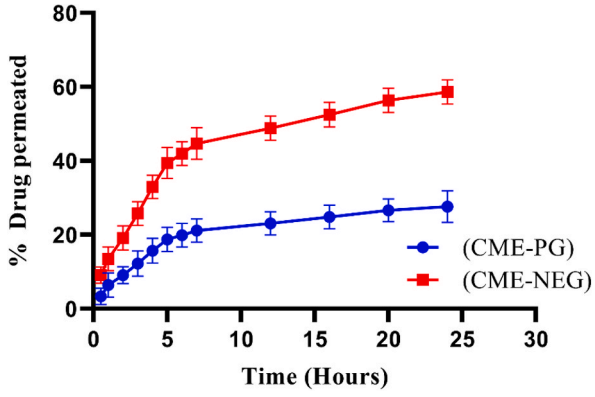

Fig. 12. Comparison of percent drug permeation of CME-NEG and CME-PG.

Table 11
In vitro permeation of CME-NEG and CME-PG.

Formulations	Permeability Coefficient (cm/h)	Flux (μg/cm^2/h)	Enhancement Ratio
CME-NEG	0.002808	16.84	2.12
CME-PG	0.001324	7.94	

viscosity upon applying force over a certain period of time. Significant differences in spreadability were observed for both formulations at various times and temperatures at the 95 % confidence interval using ANOVA. Likewise, the paired *t*-test showed significant changes (r = 0.903) between the spreadability of the CME-NEG and CME-PG.

3.11.1.5. Viscosity. In evaluating the rheological behavior of topical formulations, viscosity is a critical physical parameter that significantly affects various aspects: stability, spreadability, diffusion rate and *in vitro* drug release [67]. Viscosity data of CME-NEG and CME-PG over a time span of 90 days are presented in Fig. 10 (A, B, C, D). For both formulations, a decrease in viscosity at steady shear stress was observed during the studied time period, and this decrease was more noticeable with increasing temperature. A gel is an entangled, cross-linked network of polymer chains, which causes the viscosity of the product to increase, but when shear stress is applied, these polymeric chains tend to align themselves in the direction of flow, subsequently restoring their position through Brownian movement; thus, shear thinning behavior was observed [68]. Furthermore, as the temperature increases, there is an increase in flow, and globules increase in size and burst, which results in the lower viscosity needed for topical application to maximize absorption via viscous film [69].

3.12. In vitro release study

The *in vitro* release profile of CME extract from CME-NE, CME-NEG and CME extract solution was investigated for 24 h and results are depicted in Fig. 11. It was observed that the percentage of CME extract release after 12 h was found to be 58.39 % and 51.10 % for CME-NE and CME-NEG respectively which exceeded from the release of CME extract solution (22.48 %). After 24 h the maximum percentage of CME extract release from CME-NE, CME-NEG and CME extract solution were 93.42 %, 86.36 % and 40.55 % respectively. The finding revealed that CME-NE has higher release as compared to CME-NEG and CME extract solution. The substantial enhancement in the release of CME extract from CME-NE and CME-NEG as compared to CME extract solution is attributed to increases in the solubility and diffusion rate of poorly soluble phytobioactive constituents of CME extract due to their encapsulation in nanoemulsion formulation. Nanoemulsion has been previously reported to improve solubility and dissolution owing to small droplet size, low viscosity and the inclusion of surfactants or cosurfactants, which are among the recognized factors contributing to enhancement of drug release [70,71].

3.13. Release kinetics

Kinetic modeling approach was used to investigate the release pattern of CME extract from CME-NE, CME-NEG and CME extract solution. The release constant (R^2) values for zero order, first order, Higuchi, and Korsmeyer-Peppas (Kp) models are presented in Table 10. The findings demonstrate that the release pattern of CME extract from the CME-NE, CME-NEG and CME extract solution followed the Kp model, with R^2 values of 0.9881, 0.9896 and 0.9864, respectively. The presence of polymer and lipid layers in nanoemulsions influences the rate of CME extract release from the formulation, leading to the controlled release of CME extract. The most likely reason for the delayed release of CME extract from the nanoemulsion gel might be due to the incorporation of the Carbopol 940 polymer in the formulation, which enhances the viscosity [72]. Furthermore, prior reports suggest that nanoemulsion gel play a role as reservoir systems for the drug, starting the release of the drug first from the inner phase to the outer phase and subsequently delivering it to the targeted site of the skin [73]. In nanoemulsion gel formulation, oil droplets encapsulating the CME extract initially set free into the gel matrix and then directly penetrate into the skin's subcutaneous layer instead of transferring into the hydrophilic phase of the nanoemulsion [74]. From the proceeding discussion, it was inferred that the release of CME extract from the prepared formulations follows a diffusion control mechanism, demonstrating its potential as a controlled drug delivery system.

3.14. In vitro permeation studies

An *in vitro* permeation study was performed to assess the variation in the permeation profiles of CME extract from CME-NEG and

Table 12
In vitro Antifungal activity against Candida albicans.

Sample	Sample code	Zone of inhibition (mm)
Pure Extract	CME Extract	11.00 ± 0.13
Blank Nanoemulsion Gel	NEG	9.00 ± 0.16
CME extract Loaded Nanoemulsion Gel	CME-NEG	26.00 ± 0.11
Fluconazole	Standard	30.00 ± 0.13

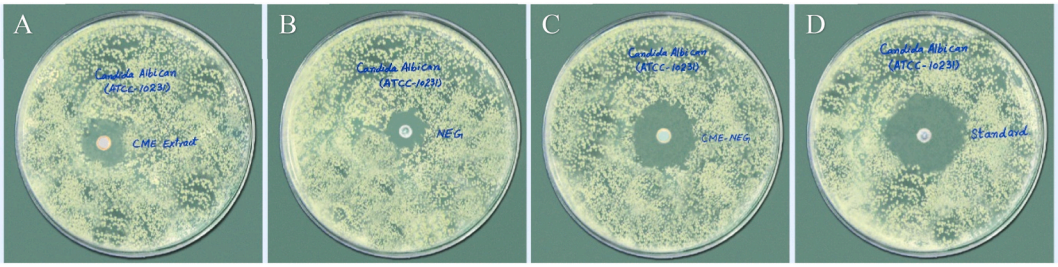

Fig. 13. *In vitro* Antifungal activity of CME Extract (A), NEG (B), CME-NEG (C) and standard (D) against Candida albicans.

CME-PG at pH 5.5 by using a Franz diffusion cell. As presented in Fig. 12, permeability of CME extract from CME-NEG was 58.63 %, which was significantly higher ($P \leq 0.05$) than CME-PG permeation (27.64 %) over the 24 h study period. The CME-NEG demonstrated an increased permeability compared to the CME-PG. The flux values for the CME-NEG and CME-PG were 16.84 μg/cm^2/h and 7.94 μg/cm^2/h, respectively. The values of flux, permeability coefficient, and enhancement ratio (E.R) are depicted in Table 11. The findings of the current study reveal that the CME-NEG demonstrated an enhancement ratio of 2.12-fold compared with the CME-PG. The observed enhancement in permeation of CME extract from the nanoemulsion was attributed to its small globule size, resulting in a larger surface area. This, in turn, led to an increase in the solubility of hydrophobic phytobioactive constituents and an increase in the rate of diffusion, which contributed to enhancing topical bioavailability and achieving the desired therapeutic outcomes [52]. Another factor contributing to the enhanced permeation offered by the CME extract encapsulated nanoemulsion gel is its lower viscosity when compared with the plain gel. It has been well documented that permeation has an inverse relationship with the viscosity of the gel; similarly, the rheological behavior of Carbopol gel also influences drug diffusion [75]. Furthermore, increased penetration may have resulted from the influence of the combined effect of formulation composition, such as surfactants, cosurfactants and oils, which make the drugs more soluble and permeable [76].

3.15. In vitro antifungal activity

The antifungal potential of CME extract, blank nanoemulsion gel, CME-NEG and fluconazole (standard) against Candida albican ATCC 10231 was evaluated using cup plate method and findings of the study are presented in Table 12 and Fig. 13 (A, B, C, D). The antifungal activity results depicted that zone of inhibition of CME-NEG (26.00 ± 0.11 mm) was greater than pure CME extract (11.00 ± 0.13 mm) against Candida albican and comparable with the standard drug (30 ± 0.13 mm). It was noticed that encapsulating the CME extract into nanoemulsion gel increased its antifungal activity. This profound antifungal activity of CME-NEG is presumed to be associated with the enhanced permeation and increase in contact area of phytobioactive constituents with fungal cells than the non-encapsulated pure plant extract [77]. Evaluating the nanoemulsion gel as a complete and functional entity rather than individual constituents allows for a more practical assessment, acknowledging the potential synergies and interactions among its constituents within the gel matrix. This approach provides insights into the overall effectiveness of the developed products in practical applications. The antifungal activity is primarily attributed to the presence of polyphenols identified in the CME extract which prevent the fungal growth by disrupting the metabolic pathways with in the fungal cells. The studies reported in literature have also demonstrated the influence of polyphenols against candida albicans [78,79] which strengthen the findings of our study. In conclusion, CME extract loaded nanoemulsion gel could be a promising alternative to traditional antifungal therapies, providing a natural and effective way to manage Candida infections.

4. Conclusion

In current study, CME-NEG was successfully fabricated. The developed nanoemulsion gel was found to be thermodynamically stable for three months, maintaining skin-friendly pH, presenting good spreadability, optimal conductivity, and viscosity. FTIR investigations confirmed the compatibility between the extract and formulation excipients. An *in vitro* permeation study showed a significant increase in the permeability coefficient and steady-state flux with an enhancement ratio of 2.12 was observed for nanoemulsion gel when compared with plain gel. Furthermore, nanoemulsion gel showed potential to overcome skin barrier properties and enhanced antifungal activity. The overall outcomes of the study showed that CME-NEG might be a promising candidate for highly effective topical delivery of phytobioactive constituents with their enhanced skin permeation and potential against skin fungal infections. The synergy between phytobioactive constituents and nanoemulsions could potentially introduce new possibilities in the realms of cosmetic and pharmaceutical industries to revolutionize the landscape of dermal drug delivery.

Ethical approval

Ethical approval was obtained from the Institutional Animal Ethics Committee (IAEC), vide IAEC No. PAEC/23/100, Faculty of Pharmacy, The Islamia University of Bahawalpur, Pakistan.

Data availability statement

Data included in article/supp. material/referenced in article.

Funding

In this research financial assistance was provided from Project Number (RSP2024R301), King Saud University, Riyadh, Saudi Arabia.

CRediT authorship contribution statement

Ambreen Akhter: Writing – original draft, Investigation, Conceptualization. **Jafir Hussain Shirazi:** Supervision, Project administration, Formal analysis, Conceptualization. **Haji Muhammad Shoaib khan:** Writing – review & editing, Validation, Supervision, Conceptualization. **Muhammad Delwar Hussain:** Visualization, Formal analysis. **Mohsin Kazi:** Writing – review & editing, Funding acquisition.

Declaration of competing interest

The authors declare that they have no known competing financial interests or personal relationships that could have appeared to influence the work reported in this paper.

Acknowledgements

The authors would like to extend their sincere appreciation to the Researchers Supporting Project Number (RSP2024R301), King Saud University, Riyadh, Saudi Arabia.

References

[1] J.L. Barbosa, et al., Development of a membrane and a bilayer of chitosan, gelatin, and polyhydroxybutyrate to be used as wound dressing for the regeneration of rat excisional wounds, J. Biomed. Mater. Res. 112 (1) (2024) 82–98.
[2] N.B. Romes, R. Abdul Wahab, M. Abdul Hamid, The role of bioactive phytoconstituents-loaded nanoemulsions for skin improvement: a review, Biotechnol. Biotechnol. Equip. 35 (1) (2021) 711–730.
[3] K. Urban, et al., The global, regional, and national burden of fungal skin diseases in 195 countries and territories: a cross-sectional analysis from the Global Burden of Disease Study 2017, JAAD international 2 (2021) 22–27.
[4] A.B.S. Duarte, et al., Antifungal activity against Candida albicans of methyl 3, 5-dinitrobenzoate loaded nanoemulsion, Braz. J. Microbiol. (2023) 1–15.
[5] R. Pereira, et al., Biofilm of Candida albicans: formation, regulation and resistance, J. Appl. Microbiol. 131 (1) (2021) 11–22.
[6] M. Rajagopal, et al., Phytochemicals and nano-phytopharmaceuticals use in skin, urogenital and locomotor disorders: are we there? Plants 11 (9) (2022) 1265.
[7] A. Noor, et al., Development and evaluation of nanoformulations containing timur oil and rosemary oil for treatment of topical fungal infections, Gels 9 (7) (2023) 516.
[8] E. Buzanello, et al., Nanoemulsions containing oil and aqueous extract of green coffee beans with antioxidant and antimicrobial activities, Nano Express 1 (1) (2020) 010058.
[9] U. Singh, et al., Compound-specific 1D 1H NMR pulse sequence selection for metabolomics analyses, ACS Omega 8 (26) (2023) 23651–23663.
[10] U. Singh, et al., Improving quality of analysis by suppression of unwanted signals through band-selective excitation in NMR spectroscopy for metabolomics studies, Metabolomics 20 (1) (2023) 7.
[11] D.J. McClements, et al., Nanoemulsion-based technologies for delivering natural plant-based antimicrobials in foods, Front. Sustain. Food Syst. 5 (2021) 35.
[12] A. Garcia-Bilbao, et al., Preparation, characterization, and biological evaluation of retinyl palmitate and Dead Sea water loaded nanoemulsions toward topical treatment of skin diseases, J. Bioact. Compat Polym. 35 (1) (2020) 24–38.
[13] R.K. Harwansh, R. Deshmukh, M.A. Rahman, Nanoemulsion: promising nanocarrier system for delivery of herbal bioactives, J. Drug Deliv. Sci. Technol. 51 (2019) 224–233.
[14] M.S. Algahtani, M.Z. Ahmad, J. Ahmad, Nanoemulsion loaded polymeric hydrogel for topical delivery of curcumin in psoriasis, J. Drug Deliv. Sci. Technol. 59 (2020) 101847.
[15] M. Kazemi, et al., Deep skin wound healing potential of lavender essential oil and licorice extract in a nanoemulsion form: biochemical, histopathological and gene expression evidences, J. Tissue Viability 29 (2) (2020) 116–124.
[16] H.H. Tayeb, et al., Nanoemulsions: formulation, characterization, biological fate, and potential role against COVID-19 and other viral outbreaks, Colloid and Interface Science Communications 45 (2021) 100533.
[17] P.A. Rocha-Filho, et al., In vitro and in vivo evaluation of nanoemulsion containing vegetable extracts, Cosmetics 4 (3) (2017) 32.
[18] S. Kumari, et al., Bioactive loaded novel nano-formulations for targeted drug delivery and their therapeutic potential, Pharmaceutics 14 (5) (2022) 1091.
[19] G. Patel, B. Prajapati, H. Hinglajia, Lipid-based drug delivery system: spotlight on nanoemulsion as versatile nanocarrier, in: Lipid-Based Drug Delivery Systems, Jenny Stanford Publishing, 2024, pp. 83–124.
[20] X. Zhang, et al., Anticancer properties of different solvent extracts of Cucumis melo L. seeds and whole fruit and their metabolite profiling using HPLC and GC-MS, BioMed Res. Int. 2020 (2020).
[21] P. Khan, N. Akhtar, Phytochemical investigations and development of ethosomal gel with Brassica oleraceae L.(Brassicaceae) extract: an innovative nano approach towards cosmetic and pharmaceutical industry, Ind. Crop. Prod. 183 (2022) 114905.
[22] S.K. Bhandary, et al., Preliminary phytochemical screening of various extracts of Punica granatum peel, whole fruit and seeds, Journal of Health and Allied Sciences NU 2 (4) (2012) 34–38.
[23] A.E. Shaffai, W.S. Mettwally, S.I. Mohamed, A comparative study of the bioavailability of Red Sea seagrass, Enhalus acoroides (Lf) Royle (leaves, roots, and rhizomes) as anticancer and antioxidant with preliminary phytochemical characterization using HPLC, FT-IR, and UPLC-ESI-TOF-MS spectroscopic analysis, Beni-Suef University Journal of Basic and Applied Sciences 12 (1) (2023) 41.
[24] W. Arshad, et al., Polymeric emulgel carrying Cinnamomum tamala extract: promising delivery system for potential topical applications, Brazilian Journal of Pharmaceutical Sciences 56 (2020).

[25] N. Iftikhar, et al., Antioxidant, anti-obesity, and hypolipidemic effects of polyphenol rich Star Anise (Illicium verum) tea in high-fat-sugar diet-induced obesity rat model, Antioxidants 11 (11) (2022) 2240.
[26] R. Tasneem, et al., Development of Phytocosmeceutical microemulgel containing flaxseed extract and its in vitro and in vivo characterization, Pharmaceutics 14 (8) (2022) 1656.
[27] U. Gul, et al., Olive oil and clove oil-based nanoemulsion for topical delivery of terbinafine hydrochloride: in vitro and ex vivo evaluation, Drug Deliv. 29 (1) (2022) 600–612.
[28] A.T. Alhamdany, A.M. Saeed, M. Alaayedi, Nanoemulsion and solid nanoemulsion for improving oral delivery of a breast cancer drug: formulation, evaluation, and a comparison study, Saudi Pharmaceut. J. 29 (11) (2021) 1278–1288.
[29] J. Ahmad, et al., Topical nano-emulgel for skin disorders: formulation approach and characterization, Recent Pat. Anti-Infect. Drug Discov. 14 (1) (2019) 36–48.
[30] M.S. Latif, et al., Formulation development and in vitro/in vivo characterization of methotrexate-loaded nanoemulsion gel formulations for enhanced topical delivery, Gels 9 (1) (2023) 3.
[31] S.A. Rashid, et al., Development, characterization and optimization of methotrexate-olive oil nano-emulsion for topical application, Pak. J. Pharm. Sci. 34 (2021).
[32] A. Mahtab, et al., Transungual delivery of ketoconazole nanoemulgel for the effective management of onychomycosis, AAPS PharmSciTech 17 (2016) 1477–1490.
[33] Z. Asghar, et al., Novel transethosomal gel containing miconazole nitrate; development, characterization, and enhanced antifungal activity, Pharmaceutics 15 (11) (2023) 2537.
[34] B. Devi, S. Singh, Phytochemical and GC-MS studies of cucumis melo L SUBSP. Agrestis (NAUDIN) PANGALO fruits, Plant Archives (09725210) 21 (1) (2021).
[35] H.M.S. Al Ubeed, et al., A comprehensive review on the techniques for extraction of bioactive compounds from medicinal cannabis, Molecules 27 (3) (2022) 604.
[36] K. Rafińska, et al., Effect of solvent and extraction technique on composition and biological activity of Lepidium sativum extracts, Food Chem. 289 (2019) 16–25.
[37] S.B. Iloki-Assanga, et al., Solvent effects on phytochemical constituent profiles and antioxidant activities, using four different extraction formulations for analysis of Bucida buceras L. and Phoradendron californicum, BMC Res. Notes 8 (1) (2015) 1–14.
[38] G.J. Molole, A. Gure, N. Abdissa, Determination of total phenolic content and antioxidant activity of Commiphora mollis (Oliv.) Engl. resin, BMC chemistry 16 (1) (2022) 48.
[39] D. Palaiogiannis, et al., Successive solvent extraction of polyphenols and flavonoids from cistus creticus L. Leaves, Oxygen 3 (3) (2023) 274–286.
[40] M.S. Ali, et al., Preparation, characterization and stability study of dutasteride loaded nanoemulsion for treatment of benign prostatic hypertrophy, Iran. J. Pharm. Res. (IJPR): IJPR 13 (4) (2014) 1125.
[41] E.M. Abdou, S.M. Kandil, H.M. El Miniawy, Brain targeting efficiency of antimigrain drug loaded mucoadhesive intranasal nanoemulsion, Int. J. Pharm. 529 (1–2) (2017) 667–677.
[42] M. Kumar, et al., Techniques for formulation of nanoemulsion drug delivery system: a review, Preventive nutrition and food science 24 (3) (2019) 225.
[43] W.A. Mahdi, et al., Product development studies of cranberry seed oil nanoemulsion, Processes 10 (2) (2022) 393.
[44] A. Azeem, et al., Nanoemulsion components screening and selection: a technical note, AAPS PharmSciTech 10 (2009) 69–76.
[45] H. Patil, J. Waghmare, Nanoemulsion: current state and perspectives, Res. J. Top. Cosmet. Sci. 4 (1) (2013) 32–40.
[46] S. Alshehri, et al., Formulation of piperine-loaded nanoemulsion: in vitro characterization, ex vivo evaluation, and cell viability assessment, ACS Omega 8 (25) (2023) 22406–22413.
[47] S. Cunha, et al., Using the quality by design (QbD) approach to optimize formulations of lipid nanoparticles and nanoemulsions: a review, Nanomed. Nanotechnol. Biol. Med. 28 (2020) 102206.
[48] S. Asadinezhad, et al., Effect of different parameters on orange oil nanoemulsion particle size: combination of low energy and high energy methods, J. Food Meas. Char. 13 (2019) 2501–2509.
[49] T. Chuacharoen, S. Prasongsuk, C.M. Sabliov, Effect of surfactant concentrations on physicochemical properties and functionality of curcumin nanoemulsions under conditions relevant to commercial utilization, Molecules 24 (15) (2019) 2744.
[50] F.A. Razzaq, et al., Glimepiride-loaded nanoemulgel; development, in vitro characterization, ex vivo permeation and in vivo antidiabetic evaluation, Cells 10 (9) (2021) 2404.
[51] N. Ullah, et al., Fabrication and optimization of essential-oil-loaded nanoemulsion using box–behnken design against staphylococos aureus and staphylococos epidermidis isolated from oral cavity, Pharmaceutics 14 (8) (2022) 1640.
[52] N. Anuar, et al., Development and characterisation of ibuprofen-loaded nanoemulsion with enhanced oral bioavailability, Heliyon 6 (7) (2020) e04570.
[53] B. Sipos, et al., Mucoadhesive meloxicam-loaded nanoemulsions: development, characterization and nasal applicability studies, Eur. J. Pharmaceut. Sci. 175 (2022) 106229.
[54] N. S Kulkarni, et al., Characterization of self-microemulsifying dosage form: special emphasis on zeta potential measurement, International Journal of Pharmaceutical & Biological Archive 10 (3) (2019) 172–179.
[55] M.R. Malik, et al., Formulation and characterization of chitosan-decorated multiple nanoemulsion for topical delivery in vitro and ex vivo, Molecules 27 (10) (2022) 3183.
[56] N. Yunitasari, et al., Phytochemical screening and metabolomic approach based on Fourier transform infrared (FTIR): identification of α-amylase inhibitor metabolites in Vernonia amygdalina leaves, J. Saudi Chem. Soc. 26 (6) (2022) 101540.
[57] P. Jain, et al., Phytochemical analysis of Mentha spicata plant extract using UV-VIS, FTIR and GC/MS technique, J. Chem. Pharmaceut. Res. 8 (2) (2016) 1–6.
[58] T. Jawaid, et al., Preparation and evaluation of nanoemulsion of Citronella essential oil with improved antimicrobial and anti-Cancer properties, Antibiotics 12 (3) (2023) 478.
[59] D.J. García, et al., Nanoemulsions for increased penetrability and sustained release of leishmanicidal compounds, Arch. Pharmazie (2023) e2300108.
[60] S. Shafiq-un-Nabi, et al., Formulation development and optimization using nanoemulsion technique: a technical note, AAPS PharmSciTech 8 (2007) E12–E17.
[61] S. Huma, et al., Development, in-vitro characterization and assessment of cosmetic potential of Beta vulgaris extract emulsion, J. Herb. Med. 23 (2020) 100372.
[62] A. Rehman, et al., Fabrication, in vitro, and in vivo assessment of eucalyptol-loaded nanoemulgel as a novel paradigm for wound healing, Pharmaceutics 14 (9) (2022) 1971.
[63] S. Baptista, F. Baptista, F. Freitas, Development of emulsions containing L-ascorbic acid and α-tocopherol based on the polysaccharide FucoPol: stability evaluation and rheological and texture assessment, Cosmetics 10 (2) (2023) 56.
[64] M. Yousuf, et al., Chemical profiling, formulation development, in vitro evaluation and molecular docking of Piper nigrum Seeds extract loaded Emulgel for anti-Aging, Molecules 27 (18) (2022) 5990.
[65] H. Khan, et al., Physical and chemical stability analysis of cosmetic multiple emulsions loaded with ascorbyl palmitate and sodium ascorbyl phosphate salts, Acta Pol. Pharm. 73 (5) (2016) 1339–1349.
[66] M.M. Almostafa, et al., Novel formulation of fusidic acid incorporated into a myrrh-oil-based nanoemulgel for the enhancement of skin bacterial infection treatment, Gels 8 (4) (2022) 245.
[67] M.S. Algahtani, et al., Thymoquinone loaded topical nanoemulgel for wound healing: formulation design and in-vivo evaluation, Molecules 26 (13) (2021) 3863.
[68] M.-S. Kwak, H.-J. Ahn, K.-W. Song, Rheological investigation of body cream and body lotion in actual application conditions, Korea Aust. Rheol. J. 27 (2015) 241–251.
[69] M. Sohail, et al., Chitosan/guar gum-based thermoreversible hydrogels loaded with pullulan nanoparticles for enhanced nose-to-brain drug delivery, Int. J. Biol. Macromol. 215 (2022) 579–595.

[70] M.S. Algahtani, M.Z. Ahmad, J. Ahmad, Nanoemulgel for improved topical delivery of retinyl palmitate: formulation design and stability evaluation, Nanomaterials 10 (5) (2020) 848.
[71] W.E. Soliman, et al., Enhancement of curcumin anti-inflammatory effect via formulation into myrrh oil-based nanoemulgel, Polymers 13 (4) (2021) 577.
[72] B. Ojha, et al., Nanoemulgel: a promising novel formulation for treatment of skin ailments, Polym. Bull. 79 (7) (2022) 4441–4465.
[73] P. Sengupta, B. Chatterjee, Potential and future scope of nanoemulgel formulation for topical delivery of lipophilic drugs, Int. J. Pharm. 526 (1–2) (2017) 353–365.
[74] Q. Ma, et al., Nanoemulgel for improved topical delivery of desonide: formulation design and characterization, AAPS PharmSciTech 22 (5) (2021) 163.
[75] M.S. Freag, Y.S. Elnaggar, O.Y. Abdallah, Development of novel polymer-stabilized diosmin nanosuspensions: in vitro appraisal and ex vivo permeation, Int. J. Pharm. 454 (1) (2013) 462–471.
[76] Z. Karami, et al., Improved oral bioavailability of repaglinide, a typical BCS Class II drug, with a chitosan-coated nanoemulsion, J. Biomed. Mater. Res. B Appl. Biomater. 108 (3) (2020) 717–728.
[77] M.E. Cecchini, et al., Nanoemulsion of Minthostachys verticillata essential oil. In-vitro evaluation of its antibacterial activity, Heliyon 7 (1) (2021) e05896.
[78] G.R. Teodoro, et al., Potential use of phenolic acids as anti-Candida agents: a review, Front. Microbiol. 6 (2015) 1420.
[79] A. Gupta, et al., Fungal endophytes: microfactories of novel bioactive compounds with therapeutic interventions; A comprehensive review on the biotechnological developments in the field of fungal endophytic biology over the last decade, Biomolecules 13 (7) (2023) 1038.